(Received 28 February 2025, Accepted 29 April 2025, Scheduled 16 May 2025)

Circular Microstrip Antenna with Electromagnetic Band Gap on Polyester Mylar Film Substrate for Metal Detection Applications in River Prawns

Watcharaphon Naktong[1], Natchayathorn Wattikornsirikul[2,*], Suwat Sakulchat[3,*], Sommart Promput[4], and Montree Kumngern[5]

[1]*Department of Telecommunication Engineering and Digital Innovation, Faculty of Engineering and Technology Rajamangala University of Technology Isan, Nakhon Ratchasima 30000, Thailand*
[2]*Department of Aircraft Maintenance Engineering, Faculty of Railway Systems and Transportation Rajamangala University of Technology Isan, Muang, Nakhon Ratchasima 30000, Thailand*
[3]*Department of Electrical Engineering, Faculty of Engineering and Architecture Rajamangala University of Technology Suvarnabhumi, Phranakhon Si Ayutthaya 13000, Thailand*
[4]*Department of Mechatronics and Robotics Engineering, School of Engineering and Innovation Rajamangala University of Technology Tawan-ok, Chonburi 20110, Thailand*
[5]*Department of Telecommunications Engineering, School of Engineering King Mongkut's Institute of Technology Ladkrabang, Bangkok 10520, Thailand*

ABSTRACT: This paper presents the design of a circular-shape microstrip patch antenna structure with nine circular Electromagnetic Band Gaps (EBGs), which have been arranged in a flower shape to increase the antenna gain and be more effective in detecting metals in river prawns. Test results show that the frequency of 1.50 GHz has the greatest effect on metal detection in river prawns. The circular microstrip antenna with the EBG structure is fabricated with a copper sheet and a thickness of 0.03 cm. The radiator patch has a radius of 1.615 cm, and the EBGs, with a radius of 0.8 cm, are arranged around a circular patch antenna structure. The substrate uses a mylar polyester film sheet that has a thickness of 0.05 cm; the dielectric value is 3.2; and the impedance bandwidth of the operating frequency range is 5.26% (1.48–1.56 GHz). This proposed antenna can increase the gain up to 43.76%, with a value of 5.19 dBi. In the application for detecting metal in river prawns, the distance for placing the Tx and Rx antennas to detect metal in river prawns is 6 cm. This circular microstrip antenna can detect metals ranging from 0.5 to 3 cm and above, with an average power value ranging from -12.38 to -18.84 dBm.

1. INTRODUCTION

Currently, giant river prawns are widely popular among consumers, being a signature dish in various restaurants and eateries. However, high-quality giant river prawns must come from rivers. The reason for giant river prawns always in demand is their excellent texture and flavor. Giant river prawns can be used as ingredients in many types of dishes and are highly nutritious, resulting in a very high domestic trade volume. Additionally, they are one of the most profitable export products, including their processing into food, which significantly increases their price [1–3]. This depends on the size of the giant river prawns, as standard giant river prawns must be longer than 15 centimeters or have a size of 5–6 pieces per kilogram. This has led to the weight tampering of giant river prawns by inserting lead or steel balls into the head area to increase the weight of the giant river prawns for sale. This issue may negatively impact the economy both domestically and in exports due to a lack of trust in the products being sold or exported. Additionally, if being used in cooking, it could pose health risks to consumers. As a result, metal detectors have developed by using electromagnetic field technology, with high-performance electronics and software capable of accurately detecting common metals [4]. These detectors are expensive; there are also maintenance issues that require long waits for spare parts from abroad, which are also expensive.

Due to the problems mentioned above, researchers have studied and designed a metal detection device for giant river prawns using the principles of high-frequency electromagnetic field technology through antenna equipment [5]. This equipment functions as a transmitter to reflect the signal back to the receiver antenna, which enhances signal reception with electromagnetic band gap (EBG) and microstrip sensors technique.

In terms of antenna arrangement and signal propagation, researchers have designed it as follows: a monopole antenna structure, a tri-band textile coplanar antenna that used the technique of 2×2 unit EBG. In this paper, a circular-shape microstrip patch antenna is designed for use with the human body, with the specific absorption rate (SAR) using the frequencies at 2.4, 3.5, and 5.8 GHz and antenna gains of 5.11, 6.43, and 7.41 dBi, respectively. In addition, the calculated SAR values of the prototype were reduced by more than 91% in the presence of EBG [6]. A circular microstrip antenna was designed at 5.9 GHz with a gain of 6.86 dBi and used in conjunction with a 3×3 unit equivalent circuit split ring resonator (EC-

* Corresponding authors: Natchayathorn Wattikornsirikul (Natchayathorn.wa@rmuti.ac.th); Suwat Sakulchat (suwat.sa@rmutsb.ac.th).

SRR), which can increase the return loss at 5.60 and 6.224 GHz and had the antenna gain of 5.58, 6.79, and 5.86 dBi, respectively [7]. A microstrip antenna with a split ring resonator (SRR) and a complementary split ring resonator (CSRR) was used for wireless applications with declination of SAR. The SRR and CSRR were placed on the radiator and used a T-shaped slot at a ground plane to achieve a hepta-band. The proposed antenna was designed for supporting frequencies of 2.4, 3.0, 3.5, 5.0, 5.8, 11.8, and 13.1 GHz, respectively, and had antenna gain of 1.94, 2.19, 1.66, 3.87, 3.65, 4.06, and 4.14 dB, respectively [8]. A circular microstrip patch antenna was designed at a frequency of 20 GHz in mode TM_{21}. A central patch was surrounded by eight circular ring antenna elements in mode TM_{11}. This antenna can enhance performance with an offset reflector, such as cross-polarization -30 dB cross-polar bandwidth, and the gain of the reflector was 41.04 dB [9].

A dual-mode, dual-band circular microstrip patch antenna was designed on a Rogers 5880 substrate for TM_{11} and TM_{01} modes. A big circular patch was implemented on the bottom and a five-ring circular stub for TM_{11} on the top. This antenna can support dual-band frequency at 2.4 GHz, 2.5% wider, and 5.2 GHz, 3.9 wider, which can increase the gain efficiency at 2.4 GHz from 6.73 dBi up to 9.55 dBi, and 5.2 GHz from 4.90 dBi up to 8.5 dBi [10]. A circle-shaped microstrip antenna was fabricated on an FR-4 substrate for wireless applications using the technique of adding four circular ring elements in TM_{11} mode. The results demonstrated an operating frequency range of 2–10 GHz with a gain of 2.4 to 10.02 dBi [11]. The microstrip patch antenna was designed with an EBG and defected ground structures (DGSs). The antenna covered resonance frequency at 10 GHz, which improved the gain and directivity up to 10.7 dBi, or about 23%, with using the square-ring slotted DGS [12]. A rectangle-shaped slot with an inverted L-shaped slit microstrip antenna was fabricated on an FR-4 substrate to enhance the impedance bandwidth with six elliptical EBG structures. It was found in the result of return loss at -10 dB that the bandwidth frequency was 36.9% (3.91–5.68 GHz) [13]. A microstrip patch antenna with 3×3 EBG was proposed for support in WiMAX applications and had an operating frequency of 5.2 GHz. The antenna was attached to an EBG with the technique of adding split ring resonator (SRR) geometry for enhancement of the antenna gain, which was placed at a distance of 4 cm and increased the gain of 3.4 dBi to 8.95 dBi [14]. The circular microstrip patch antenna was designed for MIMO applications, which were combined with shorting pin technique to control the resonant frequency by specifying TM_{11}, TM_{01}, and TM_{02} modes. The antenna had operating frequencies of 720 MHz (4.53–5.25 GHz) and 130 MHz (5.09–5.21 GHz), and antenna gain was 9.5 dBi [15]. A compact microstrip patch antenna was designed for wireless applications with an FR-4 substrate by adding ten crowns around the main circle. The antenna covered two operating frequencies in the C and Ku bands of 7.5 GHz and 17 GHz, with antenna gains of 0.8 dBi and 2.21 dBi, respectively [16]. A rectangular microstrip patch antenna with circular 2×2 array elements was fabricated for a compact size and supporting wearable MBAN devices. The proposed antenna has been used for human examination applications; the SAR decreased to 0.2281 W/kg, giving the lowest average SAR value for 1 gram of tissue [17]. A textile microstrip circular patch antenna was designed in wireless body-area network (WBAN) applications with copper and nickel coated on the upper surface with a hook-shaped etching technique. The antenna increased the four bandwidth frequencies (quad-band): 2.45 GHz, 3.32 GHz, 3.93 GHz, and 5.8 GHz, which had antenna gains of -0.81 dBi, -2.81 dBi, -1.16 dBi, and 2.83 dBi, respectively [18].

For the purpose of metal detectors and sensors, the researchers have designed the following: a microstrip metal detector (MMD) was designed for the beam profile monitoring of charged particle and synchrotron radiation beams. The results found that the profile and beam position can be accurately measured at 20 μm [19]. The circular microstrip patch antenna for gas sensors was fabricated by using the disk resonator technique. The antenna had a resonance frequency of 2.44 GHz, which examined the values of the real and imaginary parts of S_{11} compared to the ammonia concentration at 0°C to 25°C; ammonia vapor could be detected at concentrations as high as 25% [20]. A rectangular microstrip patch antenna was designed for temperature monitoring applications, which used the technique with a rectangular reflector. It was found in the test result that in an operating frequency of 5.61–5.96 GHz, it was able to measure the temperature from 40°C to 100°C, and the error was ± 2.2°C [21]. A compact microstrip patch antenna was designed for monitoring foot pressure sensing, which was measured by a frequency modulated continue wave (FMCW) generator. This antenna was combined with a vector network analyzer (VNA) in the frequency range of 5.643–5.735 GHz, and there was an error of $\pm 0.002\%$ according to the required standard [22]. A compact rectangular microstrip patch antenna was fabricated on a Rogers 5880 substrate with the operating at millimeter (mm) waves method to measure blood glucose levels. The experimental result showed that the operating frequency at 60 GHz could detect glucose concentrations as small as 1.33 mmol/l (0.025 wt%) [23]. A U-shape microstrip patch antenna was designed for moisture sensor-based use using the U-shape etching technique. The antenna covered dual-band frequencies of 5.2 GHz and 6.8 GHz, which had regression coefficients and sensitivity of 0.411/2.294 and 0.379/0.628, respectively [24]. A rectangular microstrip patch antenna was designed to detect simultaneous strain and temperature. which was implemented at the frequency of 5 GHz. The measurement results showed a strain of $17.22\mu\epsilon$ and a temperature of 0.4°C with an error of ± 0.5°C [25]. A microstrip line based method was applied to glucose detectors in noninvasive continuous monitoring by the method of main field sensing and multivariable crosschecking. The test result demonstrated the operating frequency of 1.48 GHz at 7500 μL of glucose, which found a concentration of 78 to 625 mg/dL with a sensitivity of 1.8×10^{-3} dB (mg/dL) and a concentration of 625 to 5000 mg/dL with a sensitivity of 6.6×10^{-3} dB (mg/dL) [26]. A rectangular microstrip patch antenna was applied to brain tumor detection, which used a 3×3 circular EBG at the ground plane. An antenna structure was fabricated with rubber and carbon filler material, which had an antenna gain of 4.09 dBi at the frequency of 7.3 GHz. The measurement results showed that it was able to detect brain tumors at 1.6 W/kg for SAR per 1 g

mean, which had a safety advantage for the human head [27]. A flexible square spiral-based microstrip antenna was fabricated with poly (dimethylsiloxane) material to measure water and acid contaminations in oil. The test result was demonstrated with an oil sample of 0.05% water content and a 0.5 mg KOH/g acid value, which had a deviation of only 2.88% [28]. An open-loop resonator self-complementary dipole antenna (OSCDA) was fabricated to detect a liquid adulteration based on which an impedance bandwidth of 1.1–3.3 GHz was applied. The experimental result found good sensitivity to detect adulteration in liquids, which affected the frequency range from 0.672 GHz to 2.736 GHz [29]. A microstrip line antenna was designed with adding branch microstrip line stubs and combined with split-ring resonator (SRR) and complementary SRR (CSRR) techniques. This antenna was fabricated on a polydimethylsiloxane substrate and had the purpose of detecting the temperature. The test results showed that the average sensitivity was 0.737 and could measure the temperature from 20°C to 50°C at a frequency of 2.23 GHz [30]. A wearable microstrip patch antenna was designed for measuring blood pressure using a rectangular etching technique on the antenna. The operating frequency was 2.3–2.6 GHz with a gain of 4.09 dBi. The simulation results of SAR in 10 grams of arm tissue by HFSS at power ranging from 50 to 1,000 mW showed values ranging 3.89 to 1.4917×10^3 W/kg, respectively [31]. A rectangular microstrip antenna was fabricated on FR-4 and Rogers 5880 substrates with a temperature self-compensation method for the structural crack length, which used a vertical and horizontal etching technique on the ground plane. The experimental results demonstrated that the resonant frequencies in the temperature at 20°C were f_{10} at 1.71 GHz and f_{01} at 2.35 GHz with an identification error of ± 0.2 mm within the temperature range of 0°C to 60°C [32].

According to the above research, the EBG-integrated microstrip antenna structure had advantages of increasing antenna gain but disadvantages of complex structure [12–17] and large size. In this study, the researchers focused on the structure of antennas used in combination with circular EBG plates [9–11] which had the advantage of being a basic structure. The microstrip antenna used in detecting metal for MMD [19] and other material detection antennas were applied to research on metal detection in giant river prawn [20–32]. The structural design of the microstrip antenna was circle-shaped, which combined with EBG was circle-shaped and arranged in a flower-shape. The simulation of the comparison of the properties of the microstrip antenna combined with the EBG was in Section 2. The test results of the metal detection in giant river prawns were in Section 3. A comparison of the properties of the EBG combined antenna structure with previous research is shown in Section 4. A summary of the research is shown in Section 5.

2. DESIGN AND MEASUREMENT OF MICROSTRIP ANTENNA

2.1. Microstrip Antenna Design

The design of the antenna structure has been studied with unidirectional pattern characteristics that had a simple structure and easily available materials. In the first step, rectangular and circular microstrip antenna structures were selected that can cover the entire dead river prawn body from head to tail within the temperature range of 20–30°C to measure the response frequency of the river prawns at 1.0–2.0 GHz. The microstrip antenna structures of both designs were designed and fabricated using copper sheets with a thickness (t_1, t_2) of 0.03 cm and polyester mylar film as the substrate with a thickness of (h_1) = 0.05 cm and a dielectric constant (ϵ_r) of 3.2. This polyester mylar film was used as an insulator between the radiator plate and ground plane, using a resonance frequency (f_r) of 1.50 GHz, which was the middle frequency of the response frequency range for the river prawn. The design of a rectangular microstrip antenna structure could be calculated as in Equations (1)–(5) [33–37].

$$W_1 = \frac{c}{2f_r}\sqrt{\frac{2}{\varepsilon_r + 1}} \tag{1}$$

$$\varepsilon_{eff} = \frac{\varepsilon_r + 1}{2} + (1 + 0.3h) \tag{2}$$

$$L_1 = \frac{0.22 \times c}{f_r\sqrt{\varepsilon_{eff}}} \tag{3}$$

$$W_2 = 0.45\lambda \tag{4}$$

$$L_2 = 0.65\lambda \tag{5}$$

The structure of the circular microstrip antenna could be calculated as in Equations (6)–(7) [33–37] with the radius of the circular microstrip antenna (r_1) as given in Equation (6), where F was the fringing factor for the resonance frequency (f_r) and the free space velocity of light. Calculate the radius of the ground plane (r_2) and the radius of the polyester mylar film substrate (r_3) as shown in Equation (7).

$$r_1 = \frac{F}{\left\{1 + \frac{2h}{\pi\varepsilon_r F}\left[\left(\frac{\pi F}{2h}\right) + 1.7726\right]\right\}^{1/2}} \quad : F = \frac{8.791 \times 10^9}{f_r\sqrt{\varepsilon_r}} \tag{6}$$

$$r_2 = r_3 = 0.35\lambda \tag{7}$$

Calculate the distance from the rectangular radiator plate to the polyester mylar film substrate (a_1) shown in Equation (8) and the distance from the circular radiator plate to the polyester mylar film substrate (a_2) shown in Equation (9).

$$a_1 = 0.0125\lambda \tag{8}$$

$$a_2 = 0.011\lambda \tag{9}$$

After that, the calculated values were used to simulate the antenna using the Computer Simulation Technology (CST) program, by which the values obtained from the calculations were adjusted slightly using experiential methods, as shown in Figures 1 and 2 to observe the reflection coefficient, and then both shapes of microstrip antennas were fabricated. The results obtained from the simulation were compared with measurements, as shown in Figures 3 and 4, which found that both shapes of microstrip antennas had a resonance frequency in the range of 1.47 to 1.59 GHz, which had the best coverage of wavelength range for the measurement in river prawn meat and transform in power transmission. The reflection coefficient was about -23

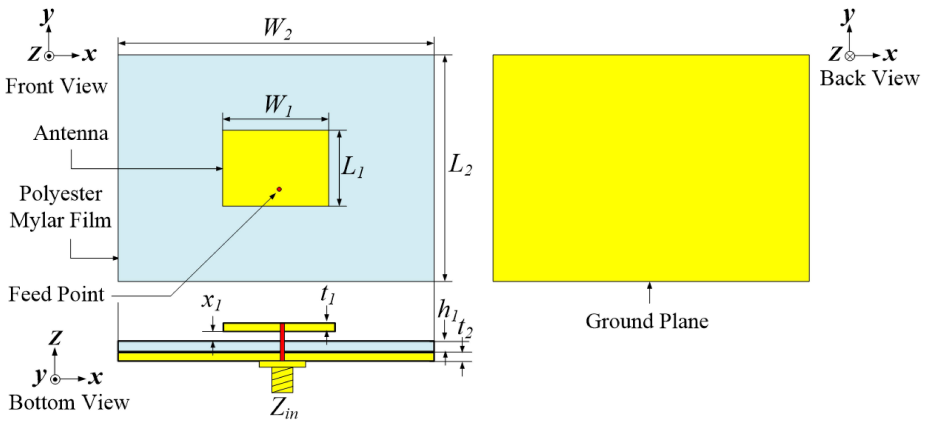

FIGURE 1. Microstrip antenna structure of rectangular microstrip antenna.

TABLE 1. Comparison of simulation and measurement results for both shapes of microstrip antennas.

Result	Antenna	f_r (GHz)	BW (GHz)
Simulation	Rectangular microstrip antenna	1.59	77.11% (0.98–2.21)
	Circular microstrip antenna	1.58	72.55% (1.01–2.16)
Measurement	Rectangular microstrip antenna	1.54	71.84% (0.99–2.10)
	Circular microstrip antenna	1.47	85.32% (0.84–2.09)

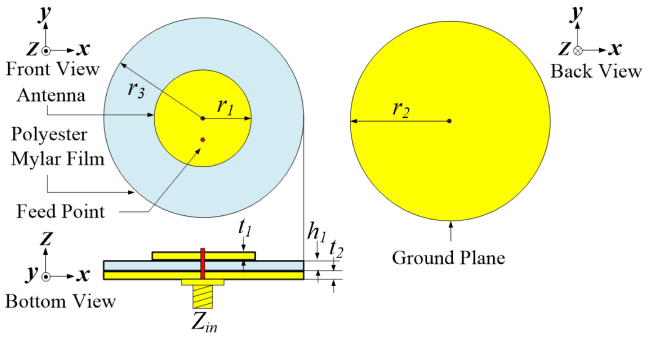

FIGURE 2. Microstrip antenna structure of circular microstrip antenna.

to −25 dB, and the impedance bandwidth covered the operating frequency range of 1.0–2.0 GHz as desired. In tuning the antenna, the technique of adjusting the distance between the radiator plate and polyester mylar film substrate was also employed, resulting in a significantly wider impedance bandwidth, as shown in Table 1.

Next, one additional rectangular microstrip antenna and one additional circular microstrip antenna were fabricated, as shown in Figure 1 and 2, to be used as the transmitting and receiving antennas for testing metal detection in river prawns measuring approximately 10–15 cm. The ball metals used for testing had a size of 0.5 cm, using the Lite VNA V2 model 64 with a frequency range of 1.0–2.0 GHz and a transmitting antenna power of −5 dBm.

River prawns were placed on the receiver antenna, with distances (d) between the transmitter and receiver antennas set at 5, 6, 7, 8, and 9 cm, and the distance from 5 to 9 cm had the greatest effect on the energy transform, as shown in Figures 5 and 7. The test results found that both shapes of microstrip antennas had a response to energy transmission covering the detection of metal in river prawns at the optimal distance (d) equal to 6 cm, which had a metal moisture content reflection value at a size of 0.5 cm and in the frequency range of 1.40–1.60 GHz. In the frequency range from 1.40 to 1.60 GHz, it was found that at a frequency of 1.50 GHz, the difference between the river prawns with a circular metal and without a circular metal was the most significant, measuring 0.81 and 1.37 dBm, respectively, as shown in Figures 6 and 8. According to the test results shown in Table 2, it could be clearly seen that the circular microstrip antenna provided a better response to energy transmission than the rectangular one.

Based on the preliminary test results for detecting metals in river prawn using the antenna in the first step, it was found that the optimal frequency range for energy transmission response was between 1.40 and 1.60 GHz, and the current density was red in the area of the radiator as shown in Figure 9(b). Moreover, in order to elicit a response to the energy transmission, the position of the river prawns must be arranged so that the metal parts were within the radius of the radiator plate, which increases complexity and consumes more time. Therefore, we need to design the antenna further to make it easier to use in the next phase. The second step was to design a circular microstrip antenna structure with a resonance frequency of 1.50 GHz, which corresponds to the highest energy transmission response. This new antenna was designed and fabricated based on the structure from Figure 9, simulated to achieve an impedance bandwidth covering the frequency range of 1.40–1.60 GHz according to the metal reflection value moisture content characteristics.

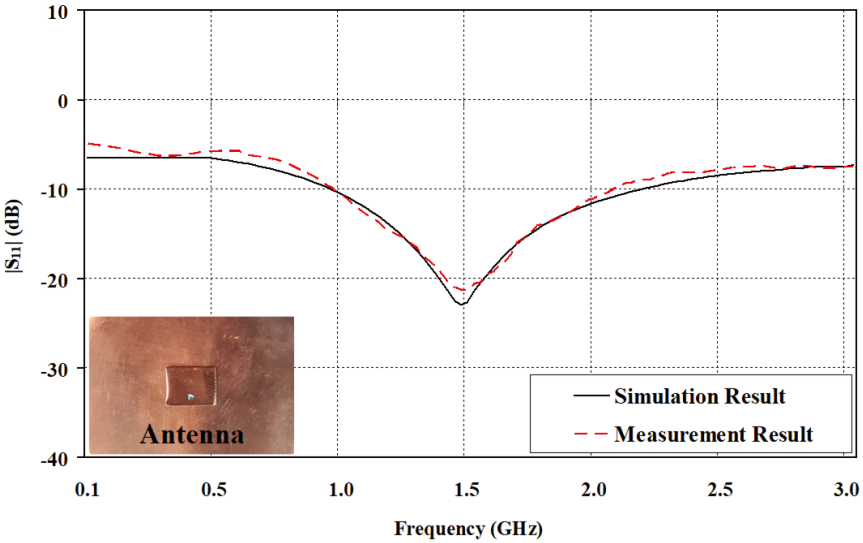

FIGURE 3. Comparison of simulation result with measurement result in the frequency range of 1.0–2.0 GHz of rectangular microstrip antenna.

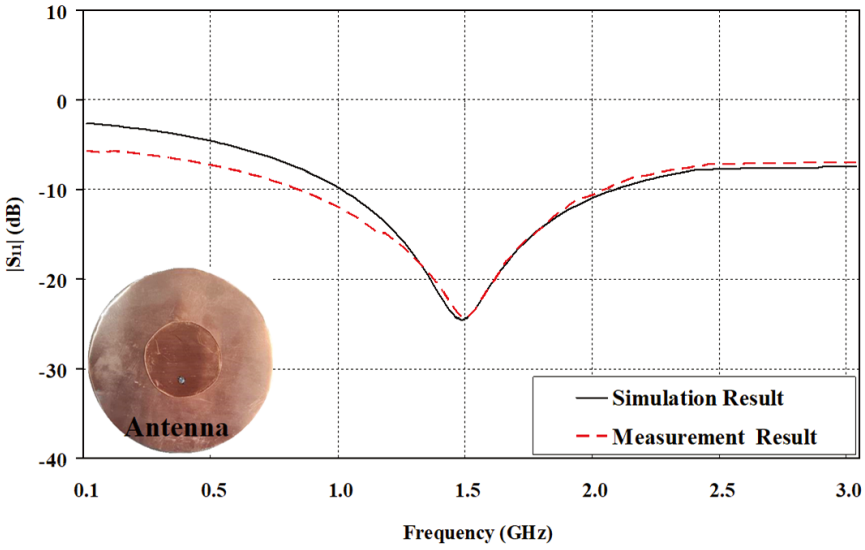

FIGURE 4. Comparison of simulation result with measurement result in the frequency range of 1.0–2.0 GHz of circular microstrip antenna.

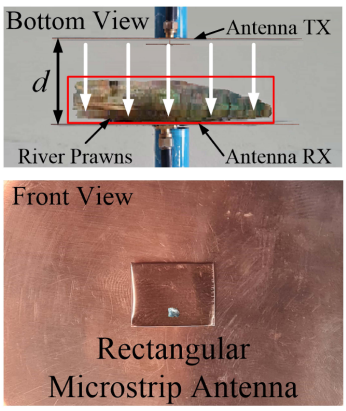

FIGURE 5. Rectangular microstrip antenna of preparing measurement.

The results from the calculations and simulations, which had been fine-tuned to achieve the optimal values, demonstrated the sizes of various parameters as shown in Table 3. Then, the second-step antenna was fabricated to measure the impedance bandwidth, which was compared with the simulation results. The resonance frequency was 1.50 GHz (1.43–1.61 GHz), which tended to be similar between the simulation and measurement results and covered the desired frequency range, as shown in Figure 9(c).

After that, we took the antenna fabricated in the second step to test for metal detection in river prawns at a frequency of 1.50 GHz with a transmission power of approximately −5 dBm once again. It was found that the issue of arranging the river prawns, which was quite complicated, could not be resolved. In the third step, the researchers solved the problem by conducting additional research on the design of circular electromag-

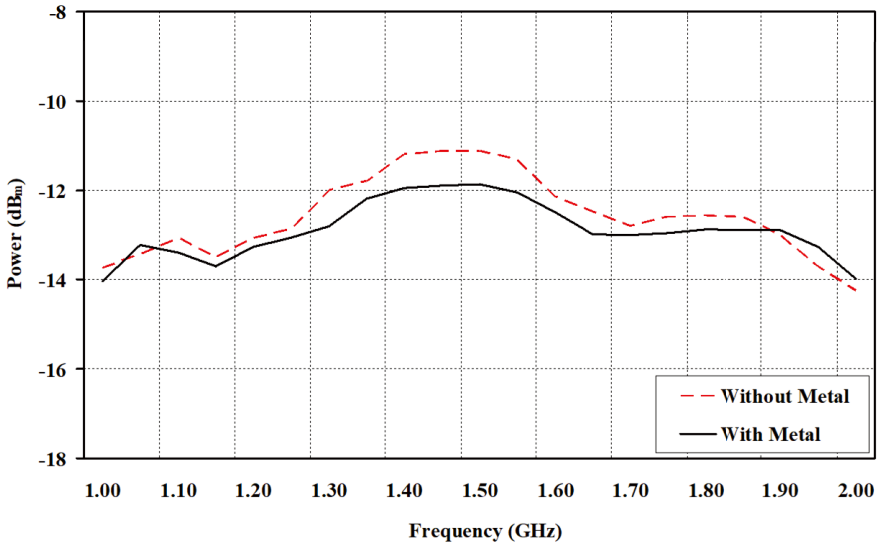

FIGURE 6. Rectangular microstrip antenna of energy transmission result.

TABLE 2. Comparison of detecting a 0.5 cm metal at a distance of 6 cm in river prawn using two shapes of microstrip antenna in the frequency range of 1.40–1.60 GHz.

Microstrip Antenna	Frequency (GHz)	Rx without metal (dBm)	Rx with metal (dBm)	Difference (dBm)
Rectangular shape	1.40	−11.48	−12.25	0.77
	1.45	−11.13	−11.87	0.74
	1.50	−11.09	−11.90	0.81
	1.55	−11.32	−12.05	0.73
	1.60	−11.69	−12.49	0.80
Circular shape	1.40	−11.10	−12.26	1.16
	1.45	−11.04	−12.35	1.31
	1.50	−11.02	−12.39	1.37
	1.55	−11.23	−12.37	1.14
	1.60	−11.32	−12.34	1.02

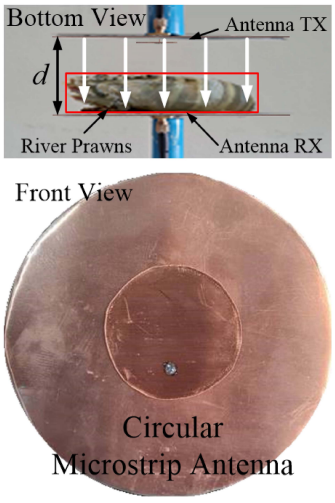

FIGURE 7. Circular microstrip antenna of preparing measurement.

netic bandgap (EBG) plates [9]. The circular EBG plates were placed around the radiator antenna as shown in Figure 10(a), which served to block the radiation pattern around the radiator patch and had current density red in the area of the radiator as shown in Figure 10(b). The antenna designed for a bandwidth of 1.50 GHz operated in the TM_{11} mode, which supported circular microstrip antennas and comprehensive measurement of the curvy body of the river prawns. All circular EBG plates had the same radius equal to r_4, serving as a reflective surface to support the TM_z mode, which was perpendicular to the radiator plate. The resonance frequency of the TM_{mnz0} mode, such as $(f_r)_{mn0}$, the resonance frequency corresponding to any TM_{mn0} mode, could be obtained from Equation (10) [10, 16].

$$(f_r)_{mn0} = \frac{1}{2\pi\sqrt{\mu\varepsilon}}\left(\frac{\chi'_{mn}}{r_1}\right) \tag{10}$$

where μ and ε are the permeability and permittivity of the surface, respectively, while r_1 is the radius of the circular plate of the radiator plate X'_{mn}.

When m and n are modes related to r_1, X'_{mn} is the derivative of the Bessel function, which helps maintain the appropriate frequency ratio to cover the bandwidth of 1.50 GHz.

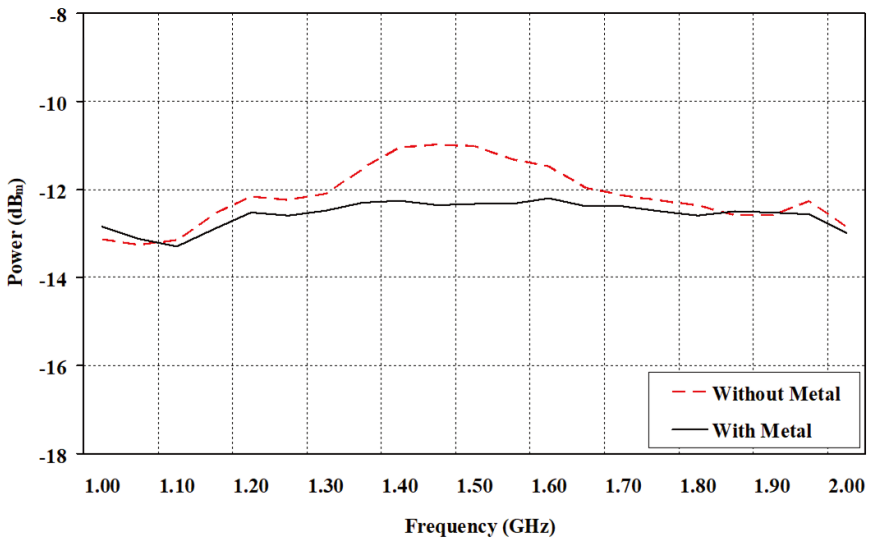

FIGURE 8. Circular microstrip antenna of energy transmission result.

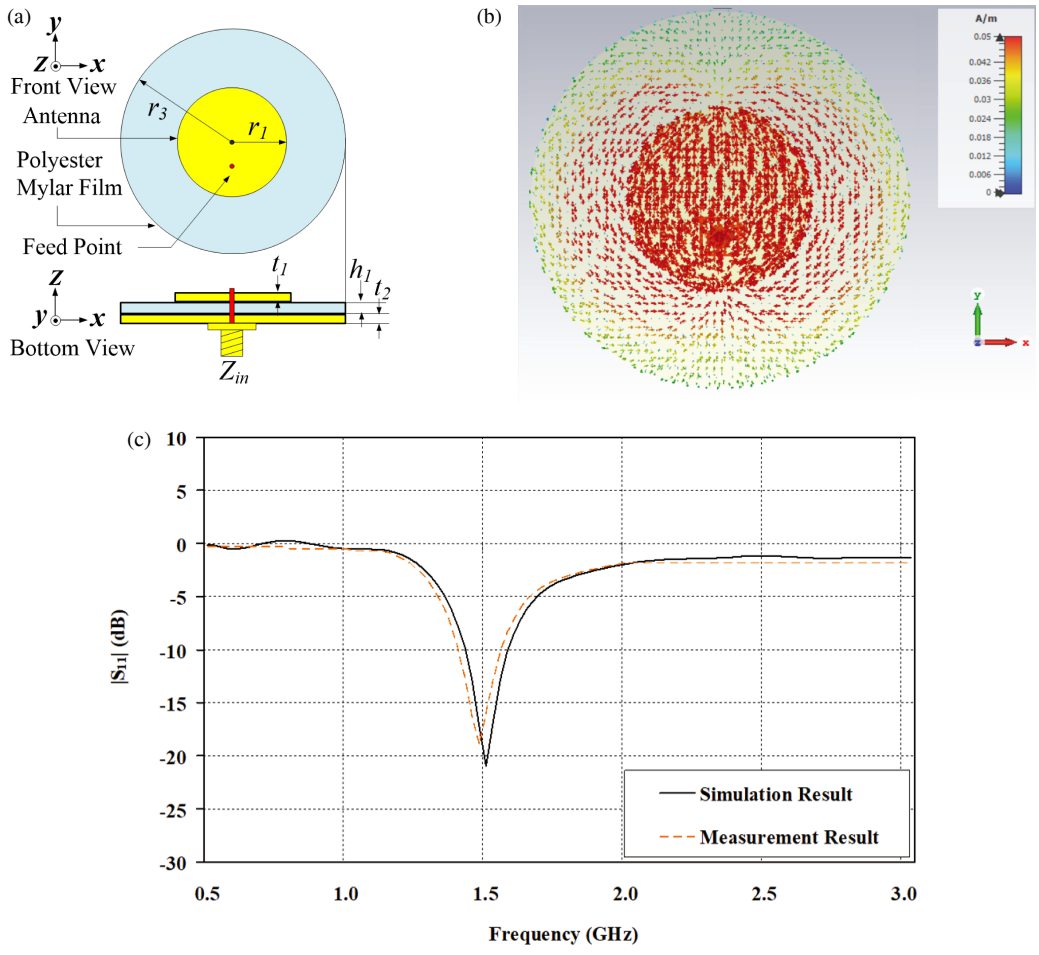

FIGURE 9. Microstrip antenna in second step (a) circular microstrip antenna (b) current density and (c) refection coefficient result of antenna.

Based on the research studies [9–11], the design of circular EBG plates should not exceed 0.5λ which would allow for optimal energy transmission. The radii of the EBG plates had a wavelength value of $0.02\lambda < r_1 < 0.05\lambda$. Therefore, the radii were tuned from 0.4 cm, 0.6 cm, 0.8 cm, and 1 cm, with the optimal value being $(r_4) = 0.8$ cm, which could be obtained from Equation (11) [36].

$$r_4 = 0.04\lambda \tag{11}$$

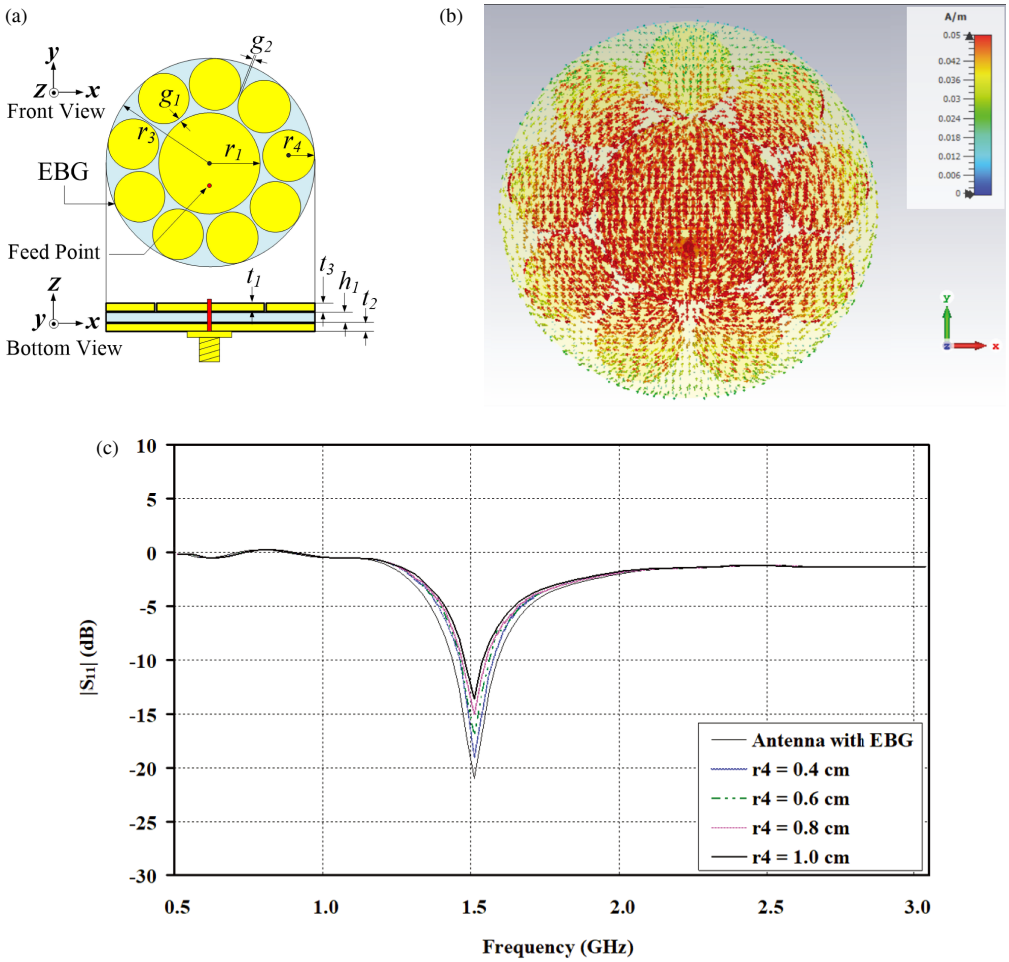

FIGURE 10. The simulation of antenna (a) circular microstrip antenna with 9 EBG plates (b) current density and (c) reflection coefficient when tuning of r_4.

TABLE 3. Parameter of rectangular and circular microstrip antennas in the first step.

Parameter	Description	Size (cm)
W_1	The width of rectangular microstrip antenna	2.112
W_2	The width of polyester mylar film	7.958
L_3	The length of rectangular microstrip antenna	1.709
L_4	The length of polyester mylar film	5.509
r_1	The radius value of circular microstrip antenna	1.615
r_2	The radius value of ground plane	5
r_3	The radius value of polyester mylar film	5
a_1	The gap between polyester mylar film and rectangular microstrip antenna	1.530
a_2	The gap between polyester mylar film and circular microstrip antenna	1.346
t_1	The thickness of circular microstrip antenna	0.03
t_2	The thickness of ground planea	0.03
h_1	The thickness of polyester mylar film	0.05

This step used the distance between the radiator plate and EBG plates ($g_1 = 0.01\lambda$), and direct variation to the distance between the EBG plates and EBG plates ($g_2 = 0.0075\lambda$), which would allow for the placement of nine EBG plates around the radiator plate, as shown in Figure 10(a), which had a bandwidth of 5.26% (1.48–1.56 GHz) as shown in Figure 10(c). The antenna gain from the wavelength of r_4 adjustment was found to be 5.08, 5.42, 5.55, and 5.34 dBi, respectively, which could be represented in a 3D radiation pattern as shown in Figure 11. The antenna gain increased to a maximum of 5.55 dBi from the

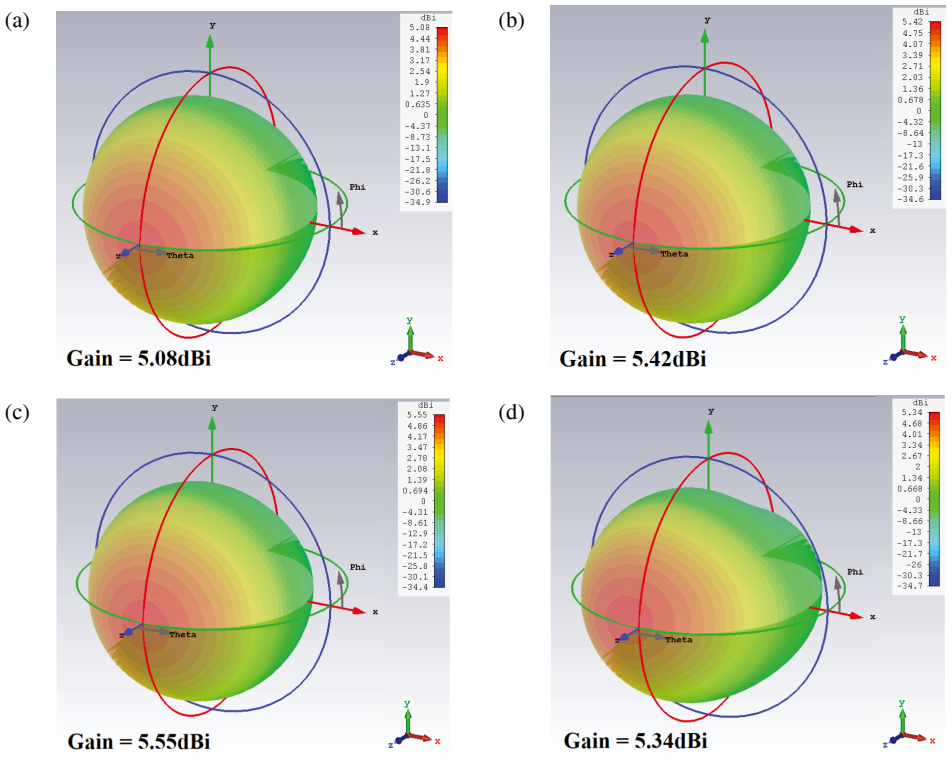

FIGURE 11. The simulation results of 3D radiation pattern (a) $r_4 = 0.4$ cm (b) $r_4 = 0.6$ cm (c) $r_4 = 0.8$ cm and (d) $r_4 = 1.0$ cm.

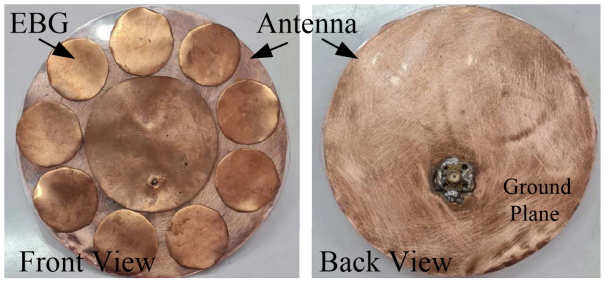

FIGURE 12. Proposed microstrip antenna of the prototype antenna.

FIGURE 13. Network analyzer model 8753ET.

TABLE 4. Comparison of simulation properties of circular microstrip antennas with EBG at 1.50 GHz.

	Circular microstrip antenna	$\lvert S_{11}\rvert$ (dB)	VSWR	Gain (dBi)	Z_{in} (Ω)
Simulation	without EBG	-20.96	$1.21:1$	3.98	$48.11 + j21.75$
	with EBG	-13.57	$1.39:1$	5.55	$54.65 - j15.09$

original 3.98 dBi, as clearly shown in Table 4, along with various parameters from the tuning adjustments in Table 5.

2.2. Measurement of Antenna Properties

After designing the circular microstrip antenna structure with nine circular EBG plates arranged in a planar antenna, it was complete. Therefore, a prototype antenna was fabricated, and its antenna properties were measured using the Network Analyzer model 8753ET, as shown in Figures 12 and 13, to measure the reflection coefficient ($|S_{11}| < -10$ dB), voltage standing wave ratio (VSWR), impedance (Z_{in}), radiation pattern, and antenna gain at a bandwidth of 1.50 GHz. The measurement results were compared with the simulation one as shown in Figure 14 and demonstrated in Table 6, which found that the values were similar, and the radiation pattern was unidirectional as shown in Figures 15 and 16.

3. EXPERIMENTAL FOR METAL DETECTION IN RIVER PRAWNS

The antenna test for detecting metals used fresh river prawns, which had sizes about 10–15 cm. The experiment was with ball metals size 0.5 cm, 1.5 cm, and bullet metal size 3 cm, by insert-

TABLE 5. Parameter of circular microstrip antennas with EBG.

Parameter	Description	Size (cm)
r_1	The radius value of circular microstrip antenna	1.615
r_2	The radius value of ground system	5
r_3	The radius value of polyester mylar film base	5
r_4	The radius value of EBG	0.8
g_1	The distance between the antenna and the EBG plate	0.2
g_2	The distance between EBG and EBG	0.15
t_1	The thickness of circular microstrip antenna	0.03
t_2	The thickness of ground system	0.03
t_3	The thickness of EBG	0.03
h_1	The thickness of polyester mylar film	0.05
d	The value of the distance between the transmitting and receiving antenna	6

TABLE 6. Simulation and measurement results comparison of circular microstrip antennas with EBG.

	Circular microstrip antenna	$\|S_{11}\|$ (dB)	VSWR	Gain (dBi)	Z_{in} (Ω)
Simulation	without EBG	-20.96	$1.21:1$	3.98	$48.11+j21.75$
	with EBG	-13.57	$1.39:1$	5.55	$54.65-j15.09$
Measurement	without EBG	-18.96	$1.30:1$	3.61	$52.57-j6.80$
	with EBG	-11.49	$1.42:1$	5.19	$59.04-j23.21$

TABLE 7. Efficiency comparison at temperatures ranging from 0–30°C.

Temperature (°C)	Input Power (mW)	Metal (cm)	Size of river prawns (cm)	Distance of Tx/Rx (cm)	Average Efficiency (%)
0–4	0.1	0.5	10–15	6	31.64
0–4	0.1	1.5	10–15	6	41.32
0–4	0.1	3.0	10–15	6	42.21
5–10	0.1	0.5	10–15	6	55.56
5–10	0.1	1.5	10–15	6	58.09
5–10	0.1	3.0	10–15	6	61.48
20–30	0.1	0.5	10–15	6	88.12
20–30	0.1	1.5	10–15	6	93.38
20–30	0.1	3.0	10–15	6	98.60

TABLE 8. The characteristic comparison of the researches.

Reference	Frequency (GHz)	Antenna and EBG shape	EBG (Unit)	Material	Size (cm)	Gain (dBi)	Applications
[9]	20	Circular	8	Arlon	1.8×0.076	41.04	-
[10]	2.45, 5.2	Circular	4	Copper	7.6×0.157	9.55, 6.93	WLAN
[11]	2–10	Circular, Ring	4	Copper	$3 \times 3 \times 0.16$	2.2-10.02	UWB
[12]	10	Rectangular, Circular	14x18	Copper	$6 \times 6.3 \times 0.152$	10.3	Wireless
[13]	4.09–4.52	L, Elliptical	2x3	Copper	$2 \times 2 \times 0.15$	3	Radio system
[14]	5.2	Octagon, Ring	3x3	Copper	$7 \times 7 \times 0.16$	8.95	WiMAX
[15]	4.53–5.25, 5.09–5.21	Circular, Circular	9	Copper	$5.6 \times 5.6 \times 0.152$	4.8	MIMO
[16]	7.5, 17	Circular, Crowns	10	Copper	$1 \times 1 \times 0.16$	0.8, 2.21	Wireless
[17]	2.37–2.39	Rectangular, Circular	25×2	Copper	$4.67 \times 5.27 \times 0.078$	-	MBAN
Proposed Antenna	1.5	Circular, Circular	9	Copper	10×0.38	5.19	Detection

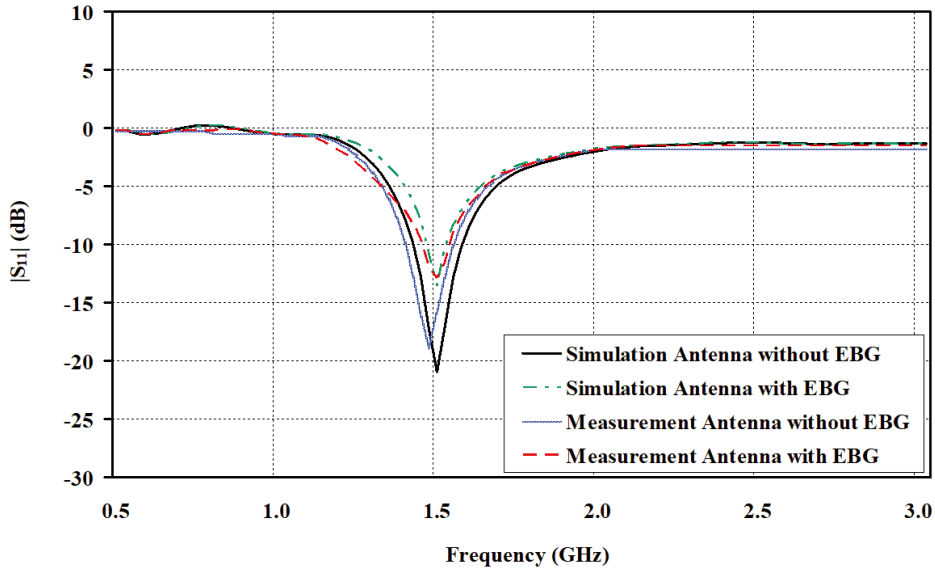

FIGURE 14. The $|S_{11}|$ (dB) comparison of simulation results and measurement results.

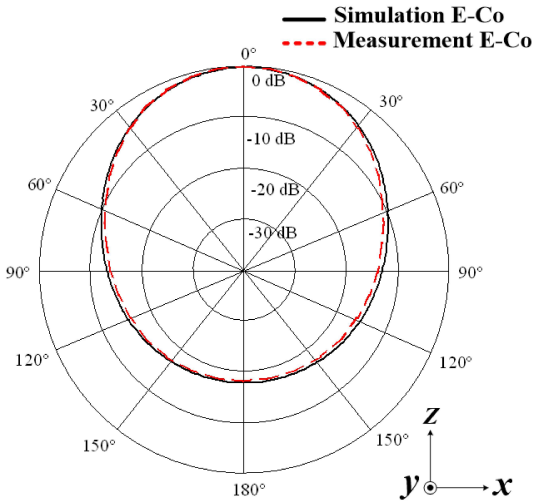

FIGURE 15. Comparison of simulation and measurement results of E-plane radiation patterns at 1.50 GHz.

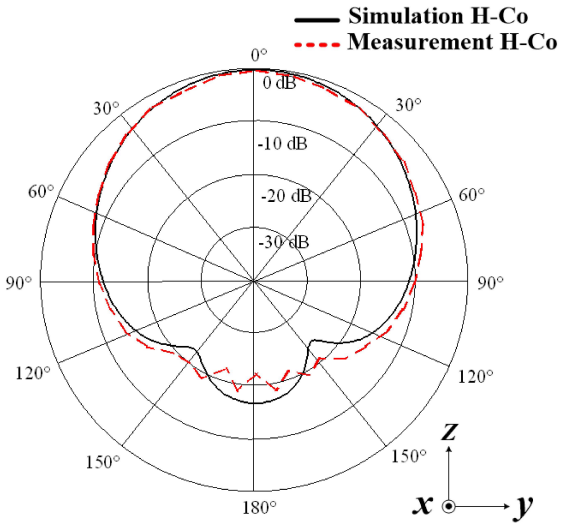

FIGURE 16. Comparison of simulation and measurement results of H-plane radiation patterns at 1.50 GHz.

ing the metals in the head and back sections of the river prawns. The power transmitter used the Lite VNA V2 model 64 [38–41] to transmit power to approximately -5 dBm, as shown in Figure 17. Microwave resonance frequency testing of a circular microstrip antenna with an EBG plate had a radius of 5 cm and a distance of 6 cm between the transmitting and receiving antennas, with 10 repetitions per experiment. The river prawns were used at temperatures ranging from 0 to 30°C. It was found that the optimal temperature for measuring the maximum average efficiency of energy transfer response was 98.60% in the range of 20 to 30°C, as shown in Table 7. Furthermore, measuring the response to energy transmission for detecting metals sized 0.5–3 cm, when river prawns were placed in various different positions, it was found that antennas can accurately detect metals, and the received energy values range from -12.38 to -18.84 dBm, respectively, as shown in Figure 18.

4. COMPARATIVE ANALYSIS

From the study and design of microstrip antenna structures with EBG plates, various antenna shapes were explored, such as circular shapes [9–11, 15, 16], rectangular shapes [12, 17], L-shape [13], and octagonal shapes [14]. Antennas had the advantage of being a simple basic shape, used in the frequency range of 2–20 GHz, resulting in varying sizes [9–17]. EBG plates were combined with antennas from 4 to 252 units [9–17], increasing the antenna gain in the range of 0.8–10.3 dBi [9–16]. In all the aforementioned researches, the focus was on applying it to wireless communication in various frequency bands [9–17]. The proposed antenna used a simple circular structure, with both radiator plate and nine EBG plates, which were chosen for the use at a frequency of 1.50 GHz with a high gain of 5.19 dBi, and was designed for focusing on metal detection

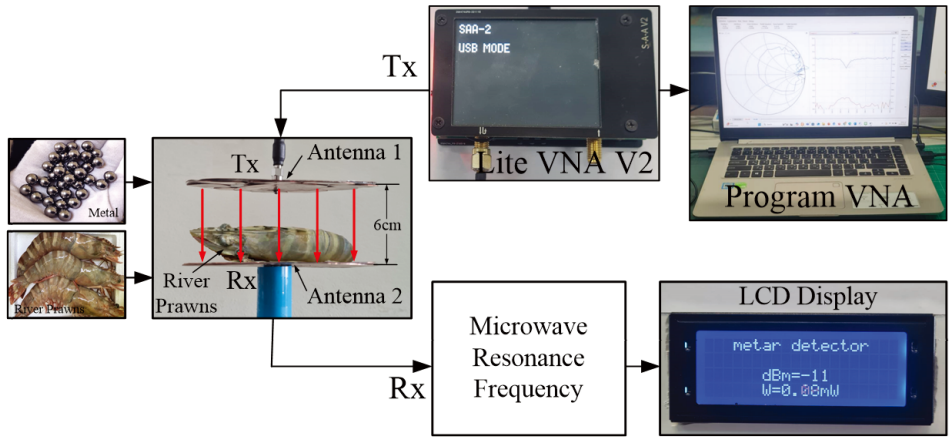

FIGURE 17. The experiment for metal detection in river prawns.

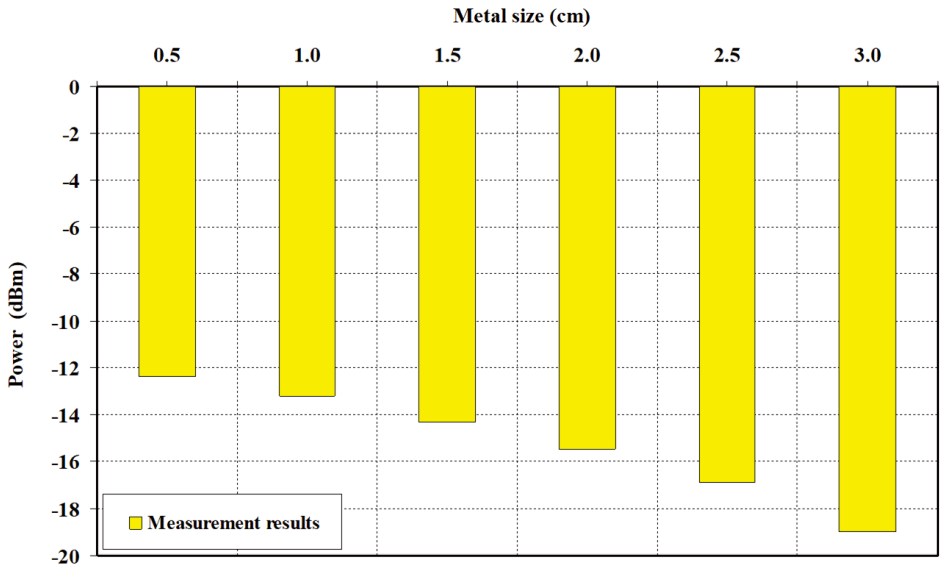

FIGURE 18. Metal detector results in river prawns.

applications. The comparison of the researches was shown in Table 8.

5. CONCLUSION

This research has designed and fabricated a circular microstrip antenna using copper sheets and a polyester mylar film sheet as the substrate between the radiator patch and the ground plane. This antenna is used in the operating frequency range of 1.50 GHz (1.48–1.56 GHz) with a gain of 3.61 dBi to be applied in detecting metals in river prawns. Preliminary test results found that improper positioning of the river prawns would prevent metal detection, causing difficulties in its application. Therefore, nine circular EBG plates were added around the radiator patch to block the radiation pattern around the radiator patch of the transmitting and receiving antennas, resulting in an increase in gain to 5.19 dBi, approximately 43.76% higher. The advantage of the EBG sheet is that it does not affect the radiation pattern changes of the antenna and has a simple design structure. Metal detection at a frequency of 1.50 GHz will use a distance of 6 cm between the transmitting and receiving antennas, with 10 repetitions per experiment. The river prawns used for testing had a temperature of approximately 20–30°C, which provided an average detection efficiency up to 98.6%. The antenna could detect metals with a radius and length ranging from 0.5 to 3 cm, with an average energy value of −12.38 to −18.84 mW. The proposed antenna can detect metals in river prawns from all sides of the arrangement with the antenna structure. Additionally, it can detect metals in river prawns at any position whether on the head or back of the river prawns, with F5 Now Co., Ltd. (Nakhon Ratchasima, Thailand) supporting research funding. Based on the results of this research, it can be applied to aquatic animals that are economically significant in Thailand and imported from abroad, such as lobsters, crabs, fish, eels, and squid, among others. This design significantly improves energy transmission efficiency and detection sensitivity while maintaining a compact structure. The gain enhancement of 43.76% (up to 5.19 dBi) demonstrates its effec-

tiveness over existing solutions. The proposed antenna structure with EBG integration is used for food safety applications and its practical impact, balancing novelty, performance, and real-world application.

ACKNOWLEDGEMENT

The authors would like to Department of Aircraft Maintenance Engineering, Faculty of Railway Systems and Transportation to support the equipment assistance, Department of Telecommunication Engineering and Digital Innovation, Faculty of Engineering and Technology to support CST Studio Suite electromagnetic simulation software, Rajamangala University of Technology Isan, Department of Electrical Engineering, Faculty of Engineering and Architecture, Rajamangala University of Technology Suvarnabhumi, and Department of Mechatronics and Robotics Engineering, School of Engineering and Innovation, Rajamangala University of Technology Tawan-ok to support the sample of raw materials and equipment, and Department of Telecommunications Engineering, School of Engineering, King Mongkut's Institute of Technology Ladkrabang to support the research successfully. Verified for practical use and received funding for machine construction from F5 Now Co., Ltd.

REFERENCES

[1] New, M. B., *Farming Freshwater Prawns: A Manual for the Culture of the Giant River Prawn (Macrobrachium Rosenbergii)*, Food & Agriculture Org., 2002.

[2] Phansawat, P., A. Keetanon, T. Rairat, P. Pichitkul, P. Poldetch, and N. Chuchird, "Benefits of male monosex culture of giant freshwater prawn (Macrobrachium rosenbergii): Improving growth performance, production yield, and profitability," *Journal of Fisheries and Environment*, Vol. 46, No. 1, 157–168, 2022.

[3] Hooper, C., P. P. Debnath, G. D. Stentiford, K. S. Bateman, K. R. Salin, and D. Bass, "Diseases of the giant river prawn Macrobrachium rosenbergii: A review for a growing industry," *Reviews in Aquaculture*, Vol. 15, No. 2, 738–758, 2023.

[4] Kladsomboon, S., C. Jaiyen, C. Choprathumma, T. Tusai, and A. Apilux, "Heavy metals contamination in soil, surface water, crops, and resident blood in Uthai District, Phra Nakhon Si Ayutthaya, Thailand," *Environmental Geochemistry and Health*, Vol. 42, 545–561, 2020.

[5] Wang, Y.-R. and H. Hao, "Design of a microstrip sensor based on a CSRR-derived structure for measuring the permittivity and permeability of materials," *Progress In Electromagnetics Research M*, Vol. 111, 235–246, 2022.

[6] El May, W., I. Sfar, J. M. Ribero, and L. Osman, "Design of low-profile and safe low SAR tri-band textile EBG-based antenna for IoT applications," *Progress In Electromagnetics Research Letters*, Vol. 98, 85–94, 2021.

[7] Zerrouk, Z. and L. Setti, "Effect of circular split ring resonator array on circular microstrip antenna used for intelligent transportation system (ITS)," *International Journal of Science and Research (IJSR)*, Vol. 9, No. 6, 45–48, 2020.

[8] Saraswat, R. K. and M. Kumar, "A metamaterial hepta-band antenna for wireless applications with specific absorption rate reduction," *International Journal of RF and Microwave Computer-Aided Engineering*, Vol. 29, No. 10, e21824, 2019.

[9] Debbarma, K. and R. Bhattacharjee, "Matched feeds for offset reflector antenna using circular microstrip patch antenna," *International Journal of RF and Microwave Computer-Aided Engineering*, Vol. 29, No. 11, e21909, 2019.

[10] Akhter, Z., R. M. Bilal, and A. Shamim, "Dual-mode circular microstrip patch antenna for airborne applications," in *2021 15th European Conference on Antennas and Propagation (EuCAP)*, 1–5, Dusseldorf, Germany, Mar. 2021.

[11] Kannadhasan, S. and R. Nagarajan, "Performance analysis of circular shape microstrip antenna for wireless communication system," in *IOP Conference Series: Materials Science and Engineering*, Vol. 1085, No. 1, 012013, 2021.

[12] Teşneli, N. B., C. Tangel, and A. Y. Teşneli, "Performance improvement of a microstrip patch antenna by using electromagnetic band gap and defected ground structures," in *2020 International Conference on Electrical, Communication, and Computer Engineering (ICECCE)*, 1–4, Istanbul, Turkey, Jun. 2020.

[13] Patil, S., A. Verma, A. K. Singh, B. K. Kanaujia, and S. Kumar, "A low-profile circularly polarized microstrip antenna using elliptical electromagnetic band gap structure," *International Journal of Microwave and Wireless Technologies*, Vol. 14, No. 8, 1009–1018, 2022.

[14] Alnaiemy, Y. and L. Nagy, "Radiation performance enhancement of a microstrip antenna based on EBG at Wi-Max bands," *UPB Science Bulletin Series*, Vol. 83, No. 3, 171–186, 2021.

[15] Deng, C., Z. Zhao, and W. Yu, "Characteristic mode analysis of circular microstrip patch antenna and its application to pattern diversity design," *IEEE Access*, Vol. 10, 2399–2407, 2021.

[16] Abdaljabar, J. S., M. Madi, A. Alhindawi, and K. Y. Kabalan, "Design and fabrication of COVID-19 microstrip patch antenna for wireless applications," *Progress In Electromagnetics Research C*, Vol. 118, 125–134, 2022.

[17] Ramanpreet, N., M. Rattan, and S. S. Gill, "Compact and low profile planar antenna with novel metastructure for wearable MBAN devices," *Wireless Personal Communications*, Vol. 118, 3335–3347, 2021.

[18] Li, H., J. Du, X.-X. Yang, and S. Gao, "Low-profile all-textile multiband microstrip circular patch antenna for WBAN applications," *IEEE Antennas and Wireless Propagation Letters*, Vol. 21, No. 4, 779–783, 2022.

[19] Pugatch, V., M. Borysova, A. Mykhailenko, O. Fedorovitch, Y. Pylypchenko, V. Perevertaylo, H. Franz, K. Wittenburg, M. Schmelling, and C. Bauer, "Micro-strip metal detector for the beam profile monitoring," *Nuclear Instruments and Methods in Physics Research Section A: Accelerators, Spectrometers, Detectors and Associated Equipment*, Vol. 581, No. 1–2, 531–534, 2007.

[20] Aloisio, D. and N. Donato, "Development of gas sensors on microstrip disk resonators," *Procedia Engineering*, Vol. 87, 1083–1086, 2014.

[21] Sanders, J. W., J. Yao, and H. Huang, "Microstrip patch antenna temperature sensor," *IEEE Sensors Journal*, Vol. 15, No. 9, 5312–5319, 2015.

[22] Yao, J., S. Tjuatja, and H. Huang, "A compact FMCW interrogator of microstrip antenna for foot pressure sensing," in *2016 Progress in Electromagnetic Research Symposium (PIERS)*, 2101–2105, Shanghai, China, Aug. 2016.

[23] Saha, S., H. Cano-Garcia, I. Sotiriou, O. Lipscombe, I. Gouzouasis, M. Koutsoupidou, G. Palikaras, R. Mackenzie, T. Reeve, P. Kosmas, and E. Kallos, "A glucose sensing system based on transmission measurements at millimetre waves using micro strip patch antennas," *Scientific Reports*, Vol. 7, No. 1, 6855, 2017.

[24] Jain, S., P. K. Mishra, V. V. Thakare, and J. Mishra, "Microstrip moisture sensor based on microstrip patch antenna," *Progress In Electromagnetics Research M*, Vol. 76, 177–185, 2018.

[25] Tchafa, F. M. and H. Huang, "Microstrip patch antenna for simultaneous strain and temperature sensing," *Smart Materials and Structures*, Vol. 27, No. 6, 065019, 2018.

[26] Huang, S. Y., Y. Yoshida, A. J. G. Inda, C. X. Xavier, W. C. Mu, Y. S. Meng, W. Yu, *et al.*, "Microstrip line-based glucose sensor for noninvasive continuous monitoring using the main field for sensing and multivariable crosschecking," *IEEE Sensors Journal*, Vol. 19, No. 2, 535–547, 2018.

[27] Ruslan, A. A., S. Y. Mohamad, N. F. A. Malek, S. H. Yusoff, S. N. Ibrahim, and F. N. M. Isa, "Design of flexible microstrip patch antenna using rubber substrate for brain tumor detection," in *2020 IEEE Student Conference on Research and Development (SCOReD)*, 1–5, Batu Pahat, Malaysia, Sep. 2020.

[28] Xue, Q., X. Tang, Y. Li, H. Liu, and X. Duan, "Contactless and simultaneous measurement of water and acid contaminations in oil using a flexible microstrip sensor," *ACS Sensors*, Vol. 5, No. 1, 171–179, 2019.

[29] Rajendran, J., S. K. Menon, and M. Donelli, "A novel liquid adulteration sensor based on a self complementary antenna," *Progress In Electromagnetics Research C*, Vol. 103, 97–110, 2020.

[30] Wu, W.-J., W.-S. Zhao, D.-W. Wang, B. Yuan, and G. Wang, "A temperature-compensated differential microstrip sensor for microfluidic applications," *IEEE Sensors Journal*, Vol. 21, No. 21, 24 075–24 083, 2021.

[31] El Abbasi, M. K., M. Madi, H. F. Jelinek, and K. Y. Kabalan, "Wearable blood pressure sensing based on transmission coefficient scattering for microstrip patch antennas," *Sensors*, Vol. 22, No. 11, 3996, 2022.

[32] Liu, Z., Y. Wang, M. Li, and Q. Guo, "Temperature self-compensation method for crack length measurement based on a microstrip antenna sensor," *IEEE Sensors Journal*, Vol. 22, No. 16, 16 036–16 045, 2022.

[33] Stutzman, W. L. and G. A. Thiele, *Antenna Theory and Design*, John Wiley & Sons, 2012.

[34] Hariyadi, T., N. Rodiah, and A. B. Pantjawati, "The effect of split ring resonator (SRR) metamaterials on the bandwidth of circular microstrip patch antennas," in *Journal of Physics: Conference Series*, Vol. 1387, No. 1, 012095, 2019.

[35] Herbko, M. and P. Lopato, "Sensitivity analysis of circular microstrip strain sensor," in *2019 International Interdisciplinary PhD Workshop (IIPhDW)*, 16–18, Wismar, Germany, May 2019.

[36] Fadhil, S. H. and R. H. Thaher, "Implementation of the GPS microstrip circular patch antenna," in *IOP Conference Series: Materials Science and Engineering*, Vol. 881, No. 1, 012144, 2020.

[37] Pradeep, P., "Design and analysis of dual-band circular patch antenna for X-band applications with enhanced bandwidth," *International Journal of Advanced Research in Science Communications and Technology (IJARSCT)*, Vol. 1, No. 1, 86–90, 2021.

[38] Naktong, W., S. Prapakarn, N. Prapakarn, and N. Wattikornsirikul, "Cantenna adjustment with 1×6 woodpile shaped EBG for application in goat manure moisture content and bulk density monitoring," *Progress In Electromagnetics Research C*, Vol. 126, 49–62, 2022.

[39] Naktong, W., K. Puangnak, N. Phanthuna, S. Prapakarn, N. Prapakarn, and N. Wattikornsirikul, "An adjusted waveguide antenna with a woodpile-shaped EBG for eucalyptus wood moisture content measurement," *Trends in Sciences*, Vol. 21, No. 6, 7645–7645, 2024.

[40] Naktong, W. and N. Wattikornsirikul, "Dipole antenna with 18×5 square electromagnetic band gap for applications used in monitoring children trapped in cars," *Progress In Electromagnetics Research M*, Vol. 112, 163–176, 2022.

[41] Promput, S., W. Naktong, and P. Thitimahatthanagusol, "Waveguide antenna study for metal detection in aquatic animals," in *15th ECTI-Conference on Innovations and Creative Technologies for Developing Smart Communities (ECTI-CARD 2023)*, Vol. 1, 475–478, Hua Hin, Thailand, 2023.